

ProPML: Probability Partial Multi-label Learning

Łukasz Struski*, Adam Pardyl^{*†‡}, Jacek Tabor* and Bartosz Zieliński^{*‡}

*Jagiellonian University, Faculty of Mathematics and Computer Science

Emails: {lukasz.struski, jacek.tabor, bartosz.zielinski}@uj.edu.pl, adam.pardyl@doctoral.uj.edu.pl

[†]Jagiellonian University, Doctoral School of Exact and Natural Sciences

[‡]IDEAS NCBR

Abstract—Partial Multi-label Learning (PML) is a type of weakly supervised learning where each training instance corresponds to a set of candidate labels, among which only some are true. In this paper, we introduce ProPML, a novel probabilistic approach to this problem that extends the binary cross entropy to the PML setup. In contrast to existing methods, it does not require suboptimal disambiguation and, as such, can be applied to any deep architecture. Furthermore, experiments conducted on artificial and real-world datasets indicate that ProPML outperforms existing approaches, especially for high noise in a candidate set.

I. INTRODUCTION

Deep neural networks are highly effective in many practical applications. However, their success is heavily dependent on the availability of a large dataset with accurate labeling. Obtaining such datasets is challenging due to the cost and discrepancies between labeling experts, like in [1], where four radiologists review each lung CT independently. Consequently, many contemporary datasets are weakly labeled, forcing researchers to propose adequate learning strategies within the Weakly Supervised Learning (WSL) paradigm [2].

Partial Multiple-label Learning (PML) [3]–[5] is a type of WSL problem where each training instance corresponds to a set of candidate labels, among which only some are true (see Figure 1). It occurs in many real-world tasks, such as sentiment analysis and document categorization [6] or classification of images, audio and video [5].

Simple PML approaches treat all candidate labels as relevant and employ the off-the-shelf multi-label image classification methods [4], [7]. However, they perform poorly because of the misleading false labels from the candidate set. Therefore, many methods adopt a disambiguation strategy, which aims to identify the relevant labels in the candidate set, e.g. using prior knowledge [8], [9] or auxiliary information [3]. They show improvement compared to simple solutions but have two issues. First, prior knowledge or auxiliary information can be inaccessible in many real-world scenarios. Second, disambiguation is usually defined on the whole dataset, which is not suitable for deep models. As a remedy, the most recent methods [5] introduce curriculum-based disambiguation with consistency regularization. However, they require complex training that alternates between learning the model and updating the disambiguation weights, which results in a suboptimal solution.



Candidate labels:

- ✓ Apple
- ✓ Banana
- Lemon
- ✓ Lime
- ✓ Orange
- Peach
- ✓ Pineapple

Fig. 1: In partial multiple-label learning, each training instance corresponds to a set of candidate labels. Only some of them are true (here, checkmarked), but we do not know which. This situation can appear, e.g., if many experts label the same image. Some of them give correct answers, while others can make mistakes.

In this paper, we introduce ProPML¹ (abbr. from Probabilistic Partial Multiple-label Learning), a novel probabilistic approach to partial multiple-label learning problems that address the above-mentioned issues. For this purpose, we establish a probability function composed of two components. The first encourages the model to find true labels in the candidate set, while the second penalizes it for predicting the labels outside of the candidate set. We show that ProPML can potentially be applied to any deep architecture and target tasks (such as classification, detection, or segmentation). Moreover, the experiments conducted on seven artificial and five real-world datasets indicate that it outperforms existing methods, especially if the number of fake labels in the candidate set increases (see Figure 2).

Therefore, our contributions can be summarized as follows:

- We introduce ProPML, a novel probabilistic approach to the PML problem, which does not require a suboptimal disambiguation strategy or other auxiliary algorithms.

¹The code of ProPML is provided together with the Supplementary Materials at <https://github.com/gmum/propml>

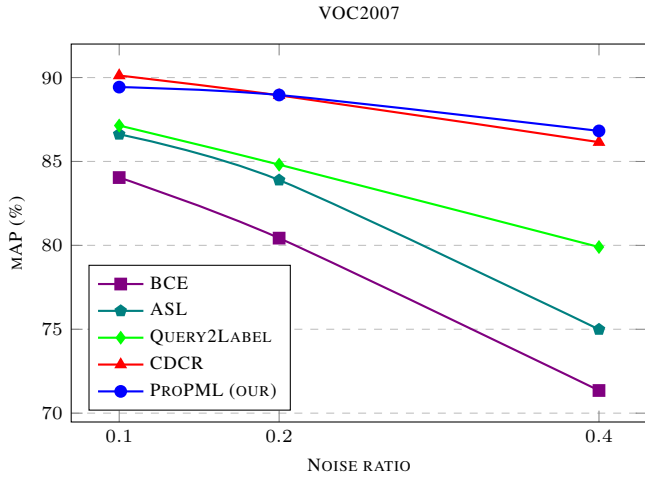


Fig. 2: The mean Average Precision (mAP) obtained for the top-5 methods on the VOC2007 dataset artificially corrupted to PML by flipping negative labels into positive with probability q (noise ratio) equals $\{0.1, 0.2, 0.4\}$. ProPML obtains outperforms existing methods for higher noise ratio. Moreover, compared to the second-best complex CDCR based on curriculum learning, ProPML requires only loss function modification.

- Our approach requires only loss function modification and, as such, can be applied to any deep architecture and any target tasks.
- We empirically prove that ProPML outperforms the existing, more composite methods, both for artificial and real-world datasets.

II. RELATED WORKS

Partial Multi-label Learning (PML) deals with noisy labels, combining two popular branches of machine learning: multi-label learning and partial-label learning (PLL) [10]–[14]. In PLL, each training instance corresponds to a set of labels among which only one is true. PML, on the other hand, extends this problem to a multi-label setup, where each training instance corresponds to a set of labels, among which some (one or more) are true.

Multiple methods have been proposed to solve the PML problem. Most of them are based on disambiguation. They try to recover the ground-truth labels from the candidate set and then use them in a standard multi-label setup. For instance, methods proposed in [15], PML-FP and PML-LC, that estimate the confidence that labels are true by exploring the structural information of feature or label space. Another approach proposed in [8] denoises the candidate labels using low-rank and sparse matrix decomposition. Method proposed in [9] estimates label confidence using either pairwise label ranking (PAR-VLS) or maximum a posteriori reasoning (PAR-MAP). More complicated approaches use two-phase disambiguation. PML-LRS [8] splits the observed label set into two label matrices, one with true and one with false labels. Then, the former is constrained to be low rank using the augmented

Lagrange multiplier algorithm [16] to prevent an overfitting method, and the second is constrained to be sparse. PML-NI [3] uses a similar technique. However, it additionally jointly learns the multi-label classifier and noisy label identifier under the supervision of the observed noise-corrupted label matrix. However, the above methods may suffer from the problem of cumulative error in the propagation process.

More recent methods move toward deep learning, like ASL [4] loss function-based approach. It dynamically down weights easy negative samples, hard thresholds (discards) the easiest ones, and removes possibly mislabeled samples. This idea was further extended in CDCR [5] with a curriculum-based disambiguation that progressively identifies ground-truth labels while incorporating the varied difficulties of different classes, such as class imbalance or easiness of distinguishing. Finally, many works transfer the PML problem to various learning scenarios, including multi-view learning [17], semi-supervised learning [18], adversarial training [19].

III. PROBABILISTIC PARTIAL MULTI-LABEL LEARNING

The main idea behind our Probability Partial Label Learning (ProPML) is to extend Binary Cross Entropy (BCE) loss to the PML setup as closely as possible. For this purpose, we establish a probability function constructed out of two components. The first one encourages the model to find true labels in the candidate set, while the second one penalizes it for predicting the labels outside of it.

To provide a detailed description of our method, let us recall that in partial multi-label learning, each training sample x corresponds to a candidate set $S \subset \{1, \dots, C\}$, which contains at least one true label and some amount of false labels (C corresponds to the number of classes). Moreover, let p_c , where $c \in C$, be the probability of predicting class c , i.e. obtaining 1 at c th output of any deep architecture. Then, our ProPML loss is defined as

$$L_{ProPML} = -\log \sum_{i \in S} p_i - \lambda \cdot \sum_{j \notin S} \log(1 - p_j), \quad (1)$$

where λ is the hyperparameter responsible for the balance between the accurate prediction of labels from S and the remaining labels, and $\sum_{i \in S} p_i \in [0, |S|]$.

To understand the idea behind ProPML, let us analyze its two components separately. The first component $-\log \sum_{i \in S} p_i$ corresponds to the labels from a candidate set, among which only some labels are true. Its value is very high if none of the candidate set labels is predicted. However, as soon as at least one label from S is predicted, the value of this component goes beyond 0 and decreases more smoothly, together with increasing sum $\sum_{i \in S} p_i$ (see Figure 3). This way, ProPML puts high pressure on predicting at least one of the candidate labels, and after that, only delicately navigates toward predicting other S labels. From this perspective, ProPML fundamentally differs from the existing PML loss functions, like ASL [4], which aims to predict all labels from a candidate set during the entire training.

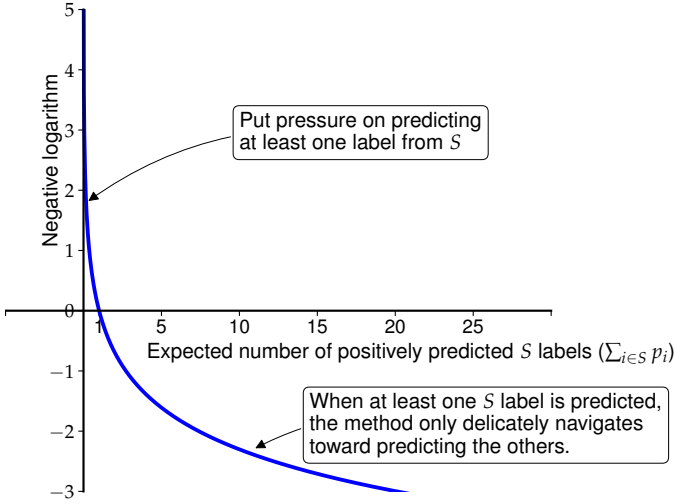


Fig. 3: The first component of ProPML loss corresponds to the expected number of positively predicted S labels. If this expected value is small, then none of the labels from S is predicted, and we put strong pressure on predicting at least one of them. However, when the expected is higher than 1, at least one label from S is probably predicted. Hence, we only delicately navigate toward predicting other S labels, which can be false. We should keep in mind that each $p_i \in [0, 1]$, therefore $\sum_{i \in S} p_i \in [0, |S|]$.

The second component $-\sum_{j \notin S} \log(1 - p_j)$ corresponds to labels outside the candidate set, which we know are all false. Therefore, this component is taken directly from BCE loss and, similarly like in BCE, it aims to prevent predicting labels from outside S .

Finally, we would like to note that when S is one element set (a single label case) and $\lambda = 1$, the ProPML loss reduces to standard BCE loss.

IV. EXPERIMENTS

In this section, we evaluate the effectiveness of ProPML by comparing its classification performance with a few existing state-of-the-art PML approaches. We used a variety of metrics to analyze the performance, including average precision, coverage loss, Hamming loss, label ranking, and one error [20]. For the first four metrics, a lower value indicates better performance. For the average precision, a higher value is better. We run the experiments on several real-world and synthetic datasets.

a) Datasets. We started with evaluating our model on five artificial datasets² corrupted to the MLP setup: Bibtext, Birds, Enron, Medical, and Scene. To obtain corrupted datasets, we first train the SVM classifier on the original labels, and then we analyze probabilities predicted by this classifier. As false labels, we take those with the highest probability (excluding originally true labels). We consider three scenarios, 50%, 100%, or 150%, depending on the

ratio of false labels to true labels. Furthermore, we use five real-world PML datasets: MIRFlickr [9], Music-emotion [21], Music-style [21], YeastBP, and YeastCC [22]. Finally, we use two vision datasets, the PASCAL Visual Object Classes Challenge 2017 (VOC2007) [23] and Microsoft Common object in Context 2014 (COCO2014) [24]. Both of them are corrupted by randomly and independently flipping negative labels into positive ones with probability q equals $\{0.1, 0.2, 0.4\}$ and $\{0.05, 0.1, 0.2\}$, respectively. All datasets are described in Table I, including the number of samples, features, classes, and the average size of a candidate set.

TABLE I: Statistics on artificial, real-world, and vision datasets show significant differences in all properties.

Dataset	Size	Dim	C	$\mathbb{E}(S)$
Artificial datasets				
Bibtex	7395	1836	159	1.23
Birds	351	260	19	1.86
Enron	1702	1001	53	3.38
Medical	978	1449	45	1.25
Scene	2407	294	6	1.07
Real-world datasets				
MIRFlickr	10433	100	7	1.77
Music-emotion	6833	98	11	2.42
Music-style	6839	98	10	1.44
YeastBP	6139	6139	217	2.22
YeastCC	6139	6139	50	3.40
Vision datasets ³				
VOC2007	9963	224×224×3	20	1.56
COCO2014	122218	224×224×3	80	2.92

b) Baseline methods. The proposed method ProPML is compared to seven state-of-the-art PML approaches. These approaches include CPLST [25], ML-kNN [26], PAR-MAP and PAR-VLS (family of PARTICLE [9]), and PML-NI [3]. CPLST is a label-embedding approach that integrates the concepts of principal component analysis and canonical correlation analysis. ML-kNN is a nearest neighbor-based multi-label classification method. PARTICLE transforms the PML task into a multi-label problem through a label propagation procedure and then induces a calibrated label ranking model. It can generate a multi-label classifier with either virtual label splitting (PAR-VLS) or maximum a posteriori inference (PAR-MAP). PML-NI uses the generation process of noisy labels in the candidate set to solve PML problems. Each of these methods has distinct advantages and disadvantages. For example, CPLST allows for integrating multiple features, while ML-kNN is simpler and easier to use.

Furthermore, for experiments on VOC2007 and COCO2014, we additionally compare ProPML to other state-of-the-art PML approaches: fPML [22] and PML-LRS [8]. Moreover, we also consider three state-of-the-art multi-label classification methods: Binary Cross Entropy (BCE), ASL [4] and Query2Label [27]. Finally, we consider the most recent curriculum disambiguation-based method CDCR [5]. fPML learns a matrix that associates instances with labels based on estimated association confidence.

²<http://mulan.sourceforge.net/datasets-mlc.html>

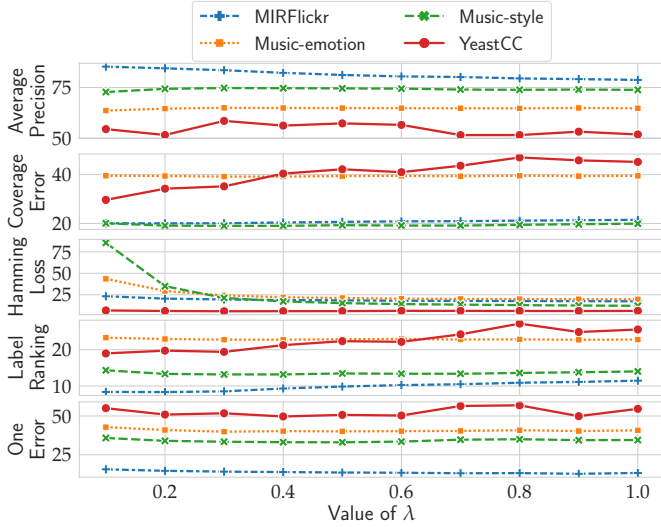


Fig. 4: Results for four real-world datasets depending on the value of the λ coefficient from the ProPML loss from Eq. (1). For average precision, the higher value, the better. For the remaining metrics, the lower value, the better. We observe a strong trend of decreasing Hamming loss for increasing λ . However, it does not generalize on other metrics, including the most important average precision, which behavior significantly differs between datasets. Nevertheless, most importantly, we observe the stability of the method for various hyperparameter values.

PML-LRS decomposes the label matrix into a ground-truth label matrix and an irrelevant label matrix, with the former constrained to be low-rank and the latter constrained to be sparse. ASL is based on the asymmetric properties of PML classification tasks, operating differently on positive and negative samples. Finally, CDCR uses highly confident prediction to create a curriculum for label disambiguation.

c) Setups. We conducted experiments in two different setups. The first setup is for relatively small artificial and real-world datasets commonly used with shallow machine-learning baseline methods. Another setup is for larger datasets, typically used with deep networks.

For smaller datasets, we use cross-validation with 80% training and 20% testing sets to demonstrate our results with standard deviations. We followed the guidelines from the original publications and applied the specified hyperparameter where possible. Moreover, we applied an MLP model with two hidden layers to our approach. The training was carried out for 500 epochs with Adam’s optimizer and stochastic gradient descent as the optimization method. We chose the parameter λ in our cost function Eq. (1) separately for each dataset using the grid search technique and narrowing it to an interval between 0.02 and 1 (see Figure 4). For large vision

³The images from the VOC2017 and COCO2014 datasets were rescaled to 224×224 in the RGB color scale to improve the processing performance of the neural network.

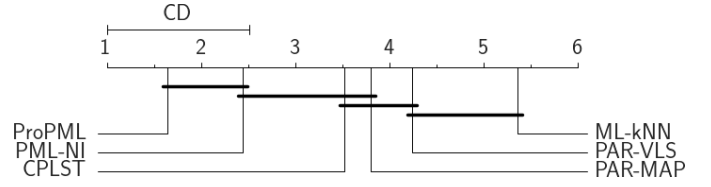


Fig. 5: Critical difference diagrams comparing results on small real-world datasets shown in Table II (smaller is better). ProPML performs significantly better than all baseline methods except PML-NI.

experiments, we use the official train-test splits. Following [4] as a backbone we employ the TResNet-L architecture [28], pretrained on the ImageNet1K dataset [29]. All images are resized to 224×224 . Moreover, as augmentation, we use standard RandAugment [30] combined with random cutout. Adam optimizer is applied with a one-cycle learning rate policy [31]. A bayesian optimization and hyperband [32] is used to tune hyper-parameters, finding the optimal learning rate between $2 \cdot 10^{-5}$ and $2 \cdot 10^{-4}$, weight decay between 10^{-7} and $5 \cdot 10^{-4}$, and the λ for ProPML function between 0.02 and 1. The exponential moving average is applied to model parameters with a decay rate of 0.9997.

All experiments were implemented using PyTorch⁴ and ran on NVIDIA GeForce RTX 3080 and Tesla V100.

V. RESULTS AND DISCUSSION.

In this section, we compare the results of our method with those of baseline approaches in two different setups of experiments for three types of datasets. We investigate how our approach fares against existing techniques and how the results vary in different scenarios.

a) The real-world datasets. Table II shows the results of the experiment conducted on real-world data. Five-fold cross-validation was used to measure the mean and variance for each method and dataset. The two highest values for each dataset and measure are highlighted, with the best result shown in bold and the second best result presented in bold italic. Our method has been regarded as the best or second-best result in 22 out of 25 cases. Moreover, it is the best in 13 out of 25 cases, with up to 3.12 gap to the second-best approach in the case of average precision and up to 1.55 gap in the case of coverage. This trend is also confirmed by the Critical Difference (CD) diagrams [33] in Figure 5, generated using all the results shown in Table II. They show that for small artificial datasets, ProPML performs significantly better than all baseline methods except PML-NI. While in the case of large datasets PML-NI method produces much worse results than our (see Tables IV and V).

In Figure 4, we observe how the results change depending on the λ parameter. There is a clear impact of this parameter on the Hamming loss. It is expected because Hamming loss is the fraction of incorrectly predicted labels. Therefore, it is

⁴<https://pytorch.org>

TABLE II: Mean results with standard deviations from five ProPML cross-validation runs on the small real-world datasets. For average precision, the higher value, the better. For the remaining metrics, the lower value, the better. The best result is shown in bold, and the second best is in bold italic. Our method has been regarded as the best or second-best result in 22 out of 25 cases. Moreover, it is the best in 13 out of 25 cases, demonstrating its effectiveness and efficiency despite its simplicity.

	Method	Average precision	Coverage	Hamming loss	Label ranking	One error
MIRFlickr	CPLST	78.67 (0.53)	22.88 (0.20)	62.66 (0.48)	12.62 (0.85)	29.48 (2.39)
	ML-kNN	69.12 (0.40)	27.07 (0.22)	76.13 (0.13)	18.43 (1.35)	45.17 (12.32)
	PAR-MAP	86.34 (0.35)	20.22 (0.09)	15.51 (0.21)	8.78 (0.10)	14.30 (0.73)
	PAR-VLS	69.39 (0.27)	26.55 (0.18)	17.34 (0.16)	20.46 (0.19)	14.00 (0.45)
	PML-NI	78.98 (0.38)	22.83 (0.15)	22.14 (0.29)	12.26 (0.22)	29.71 (1.38)
	ProPML (our)	86.24 (0.52)	20.18 (0.37)	15.98 (0.13)	8.70 (0.42)	14.57 (0.80)
Music-emotion	CPLST	61.45 (0.42)	40.82 (0.44)	77.86 (0.06)	24.36 (0.36)	46.14 (0.66)
	ML-kNN	55.27 (0.36)	46.86 (0.33)	85.05 (0.33)	30.44 (0.37)	54.65 (0.75)
	PAR-MAP	59.12 (0.50)	42.02 (0.58)	22.62 (0.24)	25.84 (0.50)	51.88 (0.86)
	PAR-VLS	61.16 (0.48)	40.93 (0.44)	21.25 (0.06)	26.08 (0.36)	42.66 (1.23)
	PML-NI	60.74 (0.24)	40.87 (0.32)	25.63 (0.78)	24.57 (0.25)	47.81 (0.70)
	ProPML (our)	64.57 (0.23)	39.45 (0.25)	20.92 (0.13)	22.61 (0.22)	39.89 (1.29)
Music-style	CPLST	73.23 (0.55)	20.56 (0.57)	85.57 (0.04)	14.53 (0.57)	34.79 (0.72)
	ML-kNN	68.33 (0.25)	26.32 (0.54)	85.62 (0.05)	19.98 (0.46)	38.18 (0.29)
	PAR-MAP	72.27 (0.53)	20.44 (0.63)	11.87 (0.21)	14.60 (0.48)	36.73 (0.68)
	PAR-VLS	72.07 (0.37)	20.35 (0.51)	11.90 (0.11)	16.44 (0.36)	35.82 (0.85)
	PML-NI	73.66 (0.45)	19.80 (0.42)	16.01 (1.92)	13.83 (0.46)	34.65 (0.71)
	ProPML (our)	75.79 (0.47)	18.25 (0.48)	12.40 (0.38)	12.38 (0.43)	31.96 (0.80)
YeastBP	CPLST	23.63 (1.31)	53.30 (0.99)	52.54 (0.42)	30.80 (0.84)	74.96 (1.65)
	ML-kNN	17.27 (1.63)	64.38 (2.30)	99.90 (0.02)	35.76 (1.25)	83.20 (2.42)
	PAR-MAP	13.19 (0.70)	65.44 (1.14)	4.83 (0.09)	38.77 (0.94)	90.63 (1.35)
	PAR-VLS	12.67 (0.42)	72.13 (0.49)	3.70 (0.04)	43.57 (0.61)	88.56 (0.59)
	PML-NI	40.06 (1.21)	40.91 (1.05)	4.24 (0.09)	21.30 (0.46)	55.77 (1.80)
	ProPML (our)	32.14 (1.27)	42.44 (1.88)	5.54 (0.78)	20.55 (0.77)	67.44 (1.40)
YeastCC	CPLST	41.02 (1.29)	37.59 (1.14)	53.48 (0.52)	26.02 (0.84)	64.46 (2.66)
	ML-kNN	30.42 (1.76)	52.30 (1.17)	99.79 (0.04)	36.37 (1.40)	75.06 (2.94)
	PAR-MAP	21.61 (0.80)	50.82 (0.83)	9.41 (0.35)	38.12 (0.90)	88.13 (0.45)
	PAR-VLS	17.78 (0.47)	63.10 (0.41)	8.28 (0.10)	48.03 (0.74)	88.74 (0.51)
	PML-NI	56.25 (1.30)	28.88 (1.42)	6.64 (0.19)	18.24 (1.16)	46.84 (1.79)
	ProPML (our)	55.37 (1.73)	28.04 (1.74)	7.20 (0.80)	18.58 (1.52)	52.42 (2.38)

calculated by summing up the number of false labels predicted as true and dividing it by the total number of labels. At the same time, the second part of the ProPML loss is also responsible for penalizing incorrectly classified false labels. Moreover, λ is a coefficient of the second component of the ProPML loss. Therefore, its increase is expected to decrease the second component and, in consequence, the Hamming loss. Unfortunately, similar trends are not observed for other metrics. Therefore, the best solution requires searching for the optimal λ . Nevertheless, most importantly, we observe the stability of the method for various hyperparameter values.

b) Artificial datasets. In Table III and the Supplementary Materials, we show results for synthetic datasets created by adding noisy labels with false to true labels ratio $q = 50\%$, 100% , and 150% . These results confirm the effectiveness of our method against the considered approaches, with up to 7.2 gap to the second-best approach in the case of average precision and up to 1.6 gap in the case of coverage. Similar to the real-world datasets, this trend is also confirmed by the Critical Difference (CD) diagrams in Figure 6, generated using all the results shown in Table III and the Supplementary Materials. Moreover, again, ProPML performs significantly better than all baseline methods except PML-NI. However,

interestingly, the gap between those two models and the remaining approaches grows together with increased q . Please, consult the Supplementary Materials to analyze the influence of parameter λ from Eq. (1) on the considered metrics.

c) Vision datasets. Table IV shows the results of our experiments on the VOC2007 dataset. As presented, our method outperforms all state-of-the-art PML approaches, as well as methods dedicated to multi-label image classification. The performance is on par with more complex, curriculum disambiguation-based CDCR, providing slightly better results in higher noise conditions, with the improvement of 0.67 percentage points in mean Average Precision (mAP) and 2.29 percentage points Class average F1 score (CF1) for $q = 0.4$. Results for COCO2014 are presented in Table V. Again our method outperforms standard PML and multi-label image classification methods. However, contrary to VOC2007, in the case of COCO2014, ProPML falls slightly behind the CDCR approach. We hypothesize that this is caused by a much larger number of possible labels (80 in COCO2014 vs. 20 in VOC2007) and a larger variance in semantic characteristics between classes making this scenario much more imbalanced. However, note that ProPML is much more straightforward than CDCR as it does not require an external curriculum-building

TABLE III: Mean results with standard deviations from five ProPML cross-validation runs on the small artificial datasets for three false to true label ratios $q = 50\%$, 100% , or 150% . For average precision, the higher value, the better. For the coverage, the lower value, the better. The results of the remaining metrics are provided in the Supplementary Materials. The best result is shown in bold, and the second best is in bold italic. Our method has been regarded as the best or second-best result in 21 out of 30 cases. Moreover, it is the best in 13 out of 30 cases, demonstrating its effectiveness and efficiency despite its simplicity.

Method	Average precision			Coverage			
	$q = 50\%$	$q = 100\%$	$q = 150\%$	$q = 50\%$	$q = 100\%$	$q = 150\%$	
Bibtex	CPLST	54.06 (0.49)	49.19 (0.69)	48.42 (0.69)	18.70 (0.83)	17.42 (0.61)	16.74 (0.26)
	ML-kNN	32.04 (0.68)	29.25 (0.76)	28.48 (0.83)	34.35 (0.40)	34.28 (0.51)	34.61 (0.45)
	PAR-MAP	19.86 (0.91)	18.13 (0.67)	16.97 (0.42)	46.30 (0.33)	46.93 (0.09)	47.31 (0.21)
	PAR-VLS	25.55 (0.25)	21.28 (0.43)	18.23 (0.54)	49.92 (0.35)	52.12 (0.42)	52.43 (0.59)
	PML-NI	54.45 (0.52)	49.54 (0.65)	48.76 (0.71)	18.00 (0.83)	16.84 (0.56)	16.19 (0.30)
	ProPML (our)	53.22 (0.64)	48.59 (0.95)	47.46 (0.64)	23.53 (0.88)	21.65 (0.54)	26.88 (0.34)
Birds	CPLST	56.25 (3.67)	53.45 (1.93)	52.25 (1.27)	29.93 (2.25)	30.06 (1.37)	30.25 (0.94)
	ML-kNN	55.66 (4.49)	51.00 (1.91)	51.16 (2.46)	27.22 (2.11)	27.66 (1.84)	27.64 (2.52)
	PAR-MAP	47.17 (2.55)	43.90 (2.06)	42.96 (1.69)	34.22 (2.85)	36.39 (3.44)	36.55 (2.33)
	PAR-VLS	57.56 (1.92)	53.00 (3.62)	49.44 (3.66)	32.78 (1.16)	36.82 (3.54)	37.30 (3.59)
	PML-NI	63.74 (1.44)	58.15 (1.97)	57.31 (2.86)	24.15 (1.27)	24.19 (1.26)	24.57 (1.23)
	ProPML (our)	66.88 (2.00)	66.77 (2.64)	62.02 (3.18)	24.35 (1.20)	22.50 (1.85)	28.13 (2.46)
Enron	CPLST	52.30 (0.83)	50.20 (0.75)	47.84 (0.52)	45.46 (1.19)	39.89 (1.43)	39.49 (0.62)
	ML-kNN	62.53 (1.48)	56.82 (0.69)	56.07 (0.70)	24.93 (0.58)	25.58 (0.75)	26.00 (0.65)
	PAR-MAP	59.29 (1.93)	50.58 (0.98)	49.68 (0.71)	28.19 (1.13)	28.03 (1.07)	27.73 (1.11)
	PAR-VLS	53.32 (2.11)	42.54 (1.80)	40.49 (0.87)	45.29 (0.93)	41.76 (1.28)	40.67 (1.88)
	PML-NI	64.35 (1.26)	61.42 (0.89)	59.72 (0.40)	32.09 (1.62)	28.41 (1.30)	27.37 (0.66)
	ProPML (our)	70.10 (1.01)	66.97 (0.50)	66.92 (0.41)	26.63 (1.11)	29.59 (1.66)	27.69 (1.02)
Medical	CPLST	79.57 (2.55)	68.06 (2.84)	67.17 (2.72)	8.12 (1.90)	7.86 (2.47)	8.70 (2.04)
	ML-kNN	80.78 (0.65)	71.05 (1.05)	70.20 (1.40)	5.78 (0.63)	6.53 (0.64)	6.57 (0.68)
	PAR-MAP	63.86 (1.46)	59.57 (1.94)	59.34 (1.44)	9.96 (0.48)	13.00 (0.62)	12.98 (0.85)
	PAR-VLS	78.07 (1.05)	63.06 (2.05)	61.00 (2.37)	11.22 (0.43)	16.97 (0.36)	17.14 (0.36)
	PML-NI	90.84 (0.52)	82.77 (1.07)	81.28 (0.79)	2.58 (0.52)	3.26 (0.33)	3.57 (0.36)
	ProPML (our)	89.19 (0.91)	77.81 (0.51)	77.47 (3.90)	3.75 (0.79)	4.71 (0.72)	4.67 (0.80)
Scene	CPLST	82.74 (2.20)	79.88 (1.66)	80.24 (1.69)	10.44 (1.73)	10.41 (1.01)	10.26 (1.03)
	ML-kNN	86.27 (1.18)	84.12 (1.09)	83.89 (1.24)	8.10 (0.52)	8.95 (0.62)	9.04 (0.74)
	PAR-MAP	85.06 (1.02)	83.87 (0.81)	84.09 (0.78)	8.61 (0.83)	9.08 (0.53)	8.89 (0.55)
	PAR-VLS	84.48 (0.80)	83.85 (0.80)	84.07 (0.82)	8.79 (0.58)	8.95 (0.55)	8.81 (0.60)
	PMLNI	84.00 (2.15)	80.68 (2.07)	80.84 (1.77)	9.56 (1.56)	9.88 (1.08)	9.83 (1.01)
	ProPML (our)	88.70 (1.08)	86.78 (1.17)	86.77 (1.01)	7.10 (0.82)	7.28 (0.74)	7.21 (0.64)

TABLE IV: Results on VOC2007 dataset for three noise ratios $q \in \{0.1, 0.2, 0.4\}$. For all metrics (presented in %), the higher value, the better. The best result is shown in bold, and the second best is in bold italic. Baseline results are presented as reported in [5]. Our method achieves the top results for the noise ratio $q \in \{0.2, 0.4\}$ and is on par with more complex CDCR for $q = 0.1$. Moreover, it is the least affected by the increase in noise ratio.

Method	$q = 0.1$			$q = 0.2$			$q = 0.4$		
	mAP	CF1	OF1	mAP	CF1	OF1	mAP	CF1	OF1
PML-NI	80.32	65.64	68.56	77.63	63.44	67.26	69.95	58.21	63.39
fPML	70.36	61.49	66.01	75.29	64.41	66.83	63.22	55.20	60.70
PMLRS	80.68	66.10	68.72	77.08	62.99	66.96	63.86	55.45	61.01
PAR-MAP	69.61	66.69	67.12	67.66	64.43	66.38	65.69	61.18	64.45
PAR-VLS	72.50	64.64	65.40	70.54	63.56	65.12	69.25	62.05	64.28
BCE	84.04	68.46	70.09	80.43	63.86	68.63	71.35	59.95	65.05
ASL	86.62	68.50	72.29	83.89	67.34	71.07	74.99	62.54	67.52
Query2Label	87.14	68.10	72.82	84.81	66.75	71.72	79.90	63.88	68.84
CDCR	90.12	71.07	72.96	88.94	70.99	73.00	86.15	70.07	71.94
ProPML (Our)	89.43	71.39	73.10	88.96	72.89	73.40	86.82	72.36	72.72
Supervised ($q = 0$)	90.93	78.77	77.06	–	–	–	–	–	–

process nor consistency regularization and can be used as a drop-in replacement for regular binary cross-entropy loss.

TABLE V: Results on COCO2014 dataset for three noise ratios $q \in \{0.1, 0.2, 0.4\}$. For all metrics (presented in %), the higher value, the better. The best result is shown in bold, and the second best is in bold italic. Baseline results are presented as reported in [5]. Our method is on par with more complex CDCR for $q = 0.05, 0.1$ and achieves slightly worse scores for $q = 0.2$. However, it is still better than other loss-based methods, such as ASL.

Method	$q = 0.05$			$q = 0.1$			$q = 0.2$		
	mAP	CF1	OF1	mAP	CF1	OF1	mAP	CF1	OF1
PML-NI	60.36	52.97	58.70	59.87	52.61	58.56	58.92	51.81	58.20
fPML	57.93	51.29	57.55	57.75	51.08	57.54	57.14	50.86	57.47
BCE	72.39	68.17	72.47	70.43	64.41	69.30	67.30	48.80	56.02
ASL	76.92	61.11	66.98	75.14	60.00	66.26	72.28	57.65	64.88
Query2Label	76.56	60.83	66.69	75.39	60.50	66.30	73.59	59.36	65.54
CDCR	77.95	73.48	77.42	77.14	72.99	77.00	76.13	72.58	76.58
ProPML (Our)	77.15	71.96	76.64	76.03	71.53	75.57	74.92	62.86	67.01
Supervised ($q = 0$)	80.23	75.03	77.75	–	–	–	–	–	–

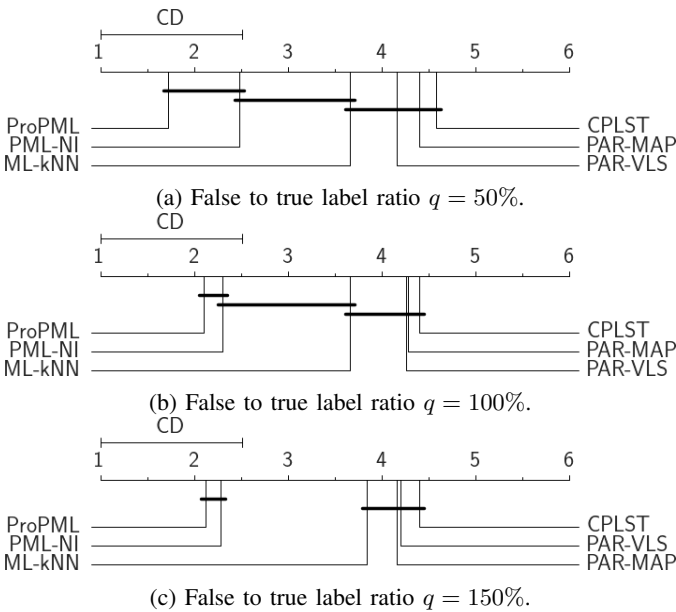


Fig. 6: Critical difference diagrams comparing results on small artificial datasets with false to true label ratio $q = 50\%$, 100% , or 150% shown in Table III and in the Supplementary Materials (smaller is better). ProPML performs significantly better than all baseline methods except PML-NI. Moreover, the gap between those two models and the remaining approaches grows together with increased q .

VI. CONCLUSIONS

In this paper, we introduced ProPML, a direct and easy-to-implement probabilistic approach to partial multi-label learning that adapts binary cross entropy to PML setup. It considers the expected value of positively predicted labels from a candidate set and uses it to encourage the model to find the true labels. As a result, it commonly overpasses the existing solutions, especially for the high number of false labels in a candidate set, as we present in multiple experiments.

In the future, we want to focus on adopting our function

to other target tasks, such as detection or segmentation, and other modalities, such as tabular data, text, sound, or graphs.

ACKNOWLEDGEMENTS

This research was partially funded by the National Science Centre, Poland, grants no. 2020/39/D/ST6/01332 (work by Łukasz Struski), 2022/47/B/ST6/03397 (work by Bartosz Zieliński), and 2021/41/B/ST6/01370 (work by Adam Pardyl and Jacek Tabor). Some experiments were performed on servers purchased with funds from a grant from the Priority Research Area (Artificial Intelligence Computing Center Core Facility) under the Strategic Programme Excellence Initiative at Jagiellonian University. We gratefully acknowledge Polish high-performance computing infrastructure PLGrid (HPC Centers: ACK Cyfronet AGH) for providing computer facilities and support within computational grant no. PLG/2022/015753.

REFERENCES

- [1] S. G. Armato III, G. McLennan, L. Bidaut, M. F. McNitt-Gray, C. R. Meyer, A. P. Reeves, B. Zhao, D. R. Aberle, C. I. Henschke, E. A. Hoffman *et al.*, “The lung image database consortium (lidc) and image database resource initiative (idri): a completed reference database of lung nodules on ct scans,” *Medical physics*, vol. 38, no. 2, pp. 915–931, 2011.
- [2] Z.-H. Zhou, “A brief introduction to weakly supervised learning,” *National Science Review*, vol. 5, no. 1, pp. 44–53, 2018.
- [3] M.-K. Xie and S.-J. Huang, “Partial multi-label learning with noisy label identification,” *IEEE Transactions on Pattern Analysis and Machine Intelligence*, vol. 44, no. 7, pp. 3676–3687, 2021.
- [4] T. Ridnik, E. Ben-Baruch, N. Zamir, A. Noy, I. Friedman, M. Protter, and L. Zelnik-Manor, “Asymmetric loss for multi-label classification,” in *Proceedings of the IEEE/CVF International Conference on Computer Vision*, 2021, pp. 82–91.
- [5] F. Sun, M.-K. Xie, and S.-J. Huang, “A deep model for partial multi-label image classification with curriculum based disambiguation,” *arXiv preprint arXiv:2207.02410*, 2022.
- [6] W. Liu, H. Wang, X. Shen, and I. W. Tsang, “The emerging trends of multi-label learning,” *IEEE transactions on pattern analysis and machine intelligence*, vol. 44, no. 11, pp. 7955–7974, 2021.
- [7] Z.-M. Chen, X.-S. Wei, P. Wang, and Y. Guo, “Multi-label image recognition with graph convolutional networks,” in *Proceedings of the IEEE/CVF conference on computer vision and pattern recognition*, 2019, pp. 5177–5186.

- [8] L. Sun, S. Feng, T. Wang, C. Lang, and Y. Jin, "Partial multi-label learning by low-rank and sparse decomposition," in *Proceedings of the AAAI conference on artificial intelligence*, vol. 33, no. 01, 2019, pp. 5016–5023.
- [9] M.-L. Zhang and J.-P. Fang, "Partial multi-label learning via credible label elicitation," *IEEE Transactions on Pattern Analysis and Machine Intelligence*, vol. 43, no. 10, pp. 3587–3599, 2020.
- [10] M.-L. Zhang, F. Yu, and C.-Z. Tang, "Disambiguation-free partial label learning," *IEEE Transactions on Knowledge and Data Engineering*, vol. 29, no. 10, pp. 2155–2167, 2017.
- [11] X. Gong, D. Yuan, and W. Bao, "Top-partial label machine," *IEEE Transactions on Neural Networks and Learning Systems*, vol. 33, no. 11, pp. 6775–6788, 2021.
- [12] Y. Yan and Y. Guo, "Partial label learning with batch label correction," in *Proceedings of the AAAI conference on artificial intelligence*, vol. 34, no. 04, 2020, pp. 6575–6582.
- [13] J. Lv, M. Xu, L. Feng, G. Niu, X. Geng, and M. Sugiyama, "Progressive identification of true labels for partial-label learning," in *International Conference on Machine Learning*. PMLR, 2020, pp. 6500–6510.
- [14] Ł. Struski, J. Tabor, and B. Zieliński, "Propall: Probabilistic partial label learning," *arXiv preprint arXiv:2208.09931*, 2022.
- [15] M.-K. Xie and S.-J. Huang, "Partial multi-label learning," in *Proceedings of the AAAI Conference on Artificial Intelligence*, vol. 32, no. 1, 2018.
- [16] Z. Lin, M. Chen, and Y. Ma, "The augmented lagrange multiplier method for exact recovery of corrupted low-rank matrices," *arXiv preprint arXiv:1009.5055*, 2010.
- [17] Z.-S. Chen, X. Wu, Q.-G. Chen, Y. Hu, and M.-L. Zhang, "Multi-view partial multi-label learning with graph-based disambiguation," in *Proceedings of the AAAI Conference on Artificial Intelligence*, vol. 34, no. 04, 2020, pp. 3553–3560.
- [18] M.-K. Xie and S.-J. Huang, "Semi-supervised partial multi-label learning," in *2020 IEEE International Conference on Data Mining (ICDM)*. IEEE, 2020, pp. 691–700.
- [19] Y. Yan and Y. Guo, "Adversarial partial multi-label learning with label disambiguation," in *Proceedings of the AAAI Conference on Artificial Intelligence*, vol. 35, no. 12, 2021, pp. 10 568–10 576.
- [20] M.-L. Zhang and Z.-H. Zhou, "A review on multi-label learning algorithms," *IEEE transactions on knowledge and data engineering*, vol. 26, no. 8, pp. 1819–1837, 2013.
- [21] M. J. Huiskes and M. S. Lew, "The mir flickr retrieval evaluation," in *Proceedings of the 1st ACM international conference on Multimedia information retrieval*, 2008, pp. 39–43.
- [22] G. Yu, X. Chen, C. Domeniconi, J. Wang, Z. Li, Z. Zhang, and X. Wu, "Feature-induced partial multi-label learning," in *2018 IEEE International Conference on Data Mining (ICDM)*. IEEE, 2018, pp. 1398–1403.
- [23] M. Everingham, L. Van Gool, C. K. Williams, J. Winn, and A. Zisserman, "The pascal visual object classes (voc) challenge," *International journal of computer vision*, vol. 88, pp. 303–308, 2009.
- [24] T.-Y. Lin, M. Maire, S. Belongie, J. Hays, P. Perona, D. Ramanan, P. Dollár, and C. L. Zitnick, "Microsoft coco: Common objects in context," in *Computer Vision—ECCV 2014: 13th European Conference, Zurich, Switzerland, September 6–12, 2014, Proceedings, Part V 13*. Springer, 2014, pp. 740–755.
- [25] Y.-N. Chen and H.-T. Lin, "Feature-aware label space dimension reduction for multi-label classification," *Advances in neural information processing systems*, vol. 25, 2012.
- [26] M.-L. Zhang and Z.-H. Zhou, "Ml-knn: A lazy learning approach to multi-label learning," *Pattern recognition*, vol. 40, no. 7, pp. 2038–2048, 2007.
- [27] S. Liu, L. Zhang, X. Yang, H. Su, and J. Zhu, "Query2label: A simple transformer way to multi-label classification," *arXiv preprint arXiv:2107.10834*, 2021.
- [28] T. Ridnik, H. Lawen, A. Noy, E. Ben Baruch, G. Sharir, and I. Friedman, "Tresnet: High performance gpu-dedicated architecture," in *proceedings of the IEEE/CVF winter conference on applications of computer vision*, 2021, pp. 1400–1409.
- [29] J. Deng, W. Dong, R. Socher, L.-J. Li, K. Li, and L. Fei-Fei, "Imagenet: A large-scale hierarchical image database," in *2009 IEEE conference on computer vision and pattern recognition*. Ieee, 2009, pp. 248–255.
- [30] E. D. Cubuk, B. Zoph, J. Shlens, and Q. V. Le, "Randaugment: Practical automated data augmentation with a reduced search space," in *Proceedings of the IEEE/CVF conference on computer vision and pattern recognition workshops*, 2020, pp. 702–703.
- [31] L. N. Smith and N. Topin, "Super-convergence: Very fast training of neural networks using large learning rates," in *Artificial intelligence and machine learning for multi-domain operations applications*, vol. 11006. SPIE, 2019, pp. 369–386.
- [32] S. Falkner, A. Klein, and F. Hutter, "Bohb: Robust and efficient hyperparameter optimization at scale," in *International Conference on Machine Learning*. PMLR, 2018, pp. 1437–1446.
- [33] J. Demšar, "Statistical comparisons of classifiers over multiple data sets," *The Journal of Machine learning research*, vol. 7, pp. 1–30, 2006.